

1 **Broad and strong memory CD4⁺ and CD8⁺ T cells induced by SARS-CoV-2 in UK**
2 **convalescent COVID-19 patients**

3
4 Yanchun Peng^{1,2†}, Alexander J. Mentzer^{3,4,20†}, Guihai Liu^{2,4,5†}, Xuan Yao^{1,2,4†}, Zixi Yin^{1,2†},
5 Danning Dong^{2,4,6†}, Wanwisa Dejnirattisai^{4†}, Timothy Rostron⁷, Piyada Supasa⁴, Chang Liu⁴,
6 Cesar Lopez-Camacho⁴, Jose Slon-campos⁴, Yuguang Zhao⁴, Dave Stuart⁴, Guido C.
7 Paesen³, Jonathan Grimes⁴, Fred Antson⁸, Oliver W. Bayfield⁸, Dorothy Hawkins⁸, De-
8 Sheng Ker⁸, Beibei Wang^{2,4}, Lance Turtle⁹, Krishanthi Subramaniam⁹, Paul Thomson⁹, Ping
9 Zhang⁴, Christina Dold¹⁰, Jeremy Ratcliff⁴, Peter Simmonds⁴, Thushan de Silva¹¹, Paul
10 Sopp⁷, Dannielle Wellington^{1,2}, Ushani Rajapaksa^{2,4}, Yi-Ling Chen¹, Mariolina Salio¹,
11 Giorgio Napolitani¹, Wayne Paes⁴, Persephone Borrow⁴, Benedikt Kessler⁴, Jeremy W.
12 Fry¹², Nikolai F. Schwabe¹², Malcolm G Semple^{13,14}, Kenneth J. Baillie¹⁵, Shona Moore⁹,
13 Peter JM Openshaw¹⁶, Azim Ansari⁴, Susanna Dunachie^{4,20}, Ellie Barnes^{4,20}, John Frater^{4,20},
14 Georgina Kerr⁴, Philip Goulder^{4,20}, Teresa Lockett¹⁷, Robert Levin¹⁸, Yonghong Zhang^{2,5},
15 Ronghua Jing⁵, Ling-Pei Ho^{1,2,4}, Oxford Immunology Network Covid-19 Response T cell
16 Consortium¹⁹, Richard J. Cornall^{1,4,20}, Chris Conlon^{2,4,20}, Paul Klenerman^{4,20}, Gavin
17 Screaton^{4,20}, Juthathip Mongkolsapaya^{2,4}, Andrew McMichael^{2,4}, Julian C. Knight^{2,3,4,20},
18 Graham Ogg^{1,2,17,20‡}, Tao Dong^{1,2,4‡*}

- 19
20 1. MRC Human Immunology Unit, MRC Weatherall Institute of Molecular Medicine,
21 University of Oxford, Oxford, U.K.
22 2. Chinese Academy of Medical Science (CAMS) Oxford Institute (COI), University of Oxford,
23 Oxford, U.K.
24 3. Wellcome Centre for Human Genetics, University of Oxford, Oxford, U.K.
25 4. Nuffield Department of Medicine, University of Oxford, Oxford, U.K.
26 5. Beijing You'an Hospital, Capital Medical University, Beijing, China
27 6. CAMS Key Laboratory of Tumor Immunology and Radiation Therapy, Xinjiang Tumor
28 Hospital, Xinjiang Medical University, China.

- 29 7. Sequencing and Flow cytometry facility, Weatherall Institute of Molecular Medicine,
30 University of Oxford, Oxford, UK
- 31 8. York Structural Biology Laboratory, Department of Chemistry, University of York, York
- 32 9. Institute of Infection and Global Health, University of Liverpool, Liverpool, UK
- 33 10. Oxford Vaccine Group, Department of Paediatrics, University of Oxford, and NIHR
34 Oxford Biomedical Research Centre, Centre for Clinical Vaccinology and Tropical Medicine,
35 University of Oxford, UK
- 36 11. Florey Institute of Host-Pathogen Interactions, Dept. of Infection, Immunity and
37 Cardiovascular Diseases, University of Sheffield, Sheffield, UK
- 38 12. ProImmune Limited, Oxford, UK
- 39 13. NIHR Health Protection Research Unit in Emerging and Zoonotic Infections, Institute of
40 Infection, Veterinary & Ecological Sciences, University of Liverpool, Liverpool, UK
- 41 14. Respiratory Medicine, Institute in The Park, Alder Hey Children's Hospital, Liverpool,
42 UK
- 43 15. Anaesthesia, Critical Care and Pain Medicine Division of Health Sciences,
44 University of Edinburgh, Edinburgh, UK
- 45 16. National Heart and Lung Institute, Faculty of Medicine, Imperial College London, London,
46 UK
- 47 17. NIHR Clinical Research Network Thames Valley & South Midlands, Oxford, UK
- 48 18. Worthing Hospital, Worthing, UK
- 49 19. Oxford Immunology Network Covid-19 Response T cell Consortium. Supplementary
50 Table 4
- 51 20. Oxford University Hospitals NHS Foundation Trust.

52 † These authors contributed equally to the work.

53 ‡ joint senior authors

54 * Correspondence author: Tao Dong (email: tao.dong@imm.ox.ac.uk)

55

56

58 **Abstract**

59 Development of SARS-CoV-2 vaccines and therapeutics will depend on understanding viral
60 immunity. We studied T-cell memory 42 patients following recovery from COVID-19 (28 mild,
61 14 severe, 16 unexposed donors), using IFN γ -based assays with peptides spanning SARS-
62 CoV-2 except ORF1. The breadth and magnitude of T-cell responses were significantly
63 higher in severe compared to mild cases. Total and spike-specific T-cell responses
64 correlated with spike-specific antibody responses. We identified 41 peptides containing
65 CD4⁺ and/or CD8⁺ epitopes, including six immunodominant regions. Six optimised CD8+
66 epitopes were defined, with peptide-MHC-pentamer-positive cells displaying central- and
67 effector-memory phenotype. **In mild cases, higher proportions of SARS-CoV-2-specific**
68 **CD8+ T-cells were observed.** The identification of T-cell responses associated with milder
69 disease, will support an understanding of protective immunity, and highlights the potential of
70 including non-spike proteins within future COVID-19 vaccine design.

71

72 **Introduction**

73

74 COVID-19 is caused by the recently emerged Severe Acute Respiratory Syndrome
75 coronavirus-2 (SARS-CoV-2). Whilst the majority of COVID-19 infections are relatively mild,
76 with recovery typically within two to three weeks^{1, 2}, a significant number of patients develop
77 severe illness, which is postulated to be related to both an overactive immune response and
78 viral-induced pathology^{3, 4}. The role of T-cell immune responses in disease pathogenesis
79 and longer-term protective immunity is currently poorly defined, but essential to understand
80 in order to inform therapeutic interventions and vaccine design.

81

82 Currently, there are many ongoing vaccine trials, but it is unknown whether they will provide
83 long lasting protective immunity. Most vaccines are designed to induce antibodies to the
84 SARS-CoV-2 spike protein, but it is not yet known if this will be sufficient to induce full
85 protective immunity to SARS-CoV-2^{5,6, 7,8}. Studying natural immunity to the virus, including
86 the role of SARS-CoV-2-specific T-cells is critical to fill the current knowledge gaps for
87 improved vaccine design.

88

89 For many primary virus infections, it typically takes 7-10 days to prime and expand adaptive
90 T-cell immune responses in order to control the virus⁹. This coincides with the typical time it
91 takes for COVID-19 patients to either recover or develop severe illness. There is an
92 incubation time of 4-7 days before symptom onset, and a further 7-10 days before
93 individuals progress to severe disease¹⁰. Such a pattern of progression raises the possibility
94 that a poor T cell response contributes to SARS-CoV-2 viral persistence and COVID-19
95 mortality, whereas strong T cell responses are protective in the majority of individuals.

96

97 Evidence supporting a role for T cells in COVID-19 protection and pathogenesis is currently
98 incomplete and sometimes conflicting^{3,11,12,13,14}. To date there have been few studies
99 analysing SARS-CoV-2-specific T-cell responses and their role in disease progression¹⁵,

100 although virus specific T cells have been shown to be protective in human influenza
101 infection¹⁶. In a study of CD4⁺ and CD8⁺ T-cell responses to SARS-CoV-2 in non-
102 hospitalised convalescent subjects, Grifoni *et al* found that all recovered subjects
103 established CD4⁺ responses and 70% established CD8⁺ memory responses to SARS-CoV-
104 2¹⁷. SARS-CoV-2-specific CD4⁺ T-cell responses were also frequently observed in
105 unexposed subjects in their study, suggesting the possibility of pre-existing cross-reactive
106 immune memory to seasonal coronaviruses. In Singapore, Le Bert *et al*¹⁸ found long lasting
107 T cell immunity to the original SARS coronavirus nucleoprotein (NP) in those that were
108 infected in 2003. These T cells cross-reacted with SARS-CoV-2 NP, and T cells cross
109 reactive with NSP7 and NSP13 of other coronaviruses were also present in those
110 uninfected with either SARS coronaviruses¹⁸.

111

112 In the present study, the overall and immunodominant SARS-CoV-2-specific memory T-cell
113 response in subjects who had recovered from COVID-19 were evaluated *ex vivo* using
114 peptides spanning the full proteome of the SARS-CoV-2, except for ORF-1. Epitopes were
115 identified using two-dimensional matrix peptide pools and CD4⁺ and CD8⁺ T cell responses
116 were distinguished. The epitope specificity and HLA restriction of the dominant CD8⁺ T-cell
117 responses were defined in *ex vivo* assays and using *in vitro* cultured short-term T-cell lines.
118 The *ex vivo* functions of SARS-CoV-2-specific T-cells specific for dominant epitopes were
119 evaluated by their intracellular cytokine production profiles. Broad, and frequently strong,
120 SARS-CoV-2 specific CD4⁺ and CD8⁺ T-cell responses were seen in the majority of
121 convalescent patients, with significantly larger overall T-cell responses in those that had
122 severe compared to mild disease. However, there was a greater proportion of CD8⁺ T-cell
123 compared to CD4⁺ T cell responses in mild cases with higher frequencies of multi-cytokine
124 production by matrix (M) and nucleoprotein (NP)-specific CD8⁺ T-cells.

125 **Results:**

126

127 **Study subjects**

128 42 individuals were recruited following recovery from COVID-19, including 28 mild cases and
129 14 severe cases. In addition, 16 control individuals sampled in 2017-2019, before COVID-19
130 appeared, were studied in parallel. Supplementary Fig. 1 shows the participant
131 characteristics. No significant differences in gender or age were noted between mild and
132 severe groups. The SaO₂/FiO₂ ratio in severe cases ranged from 4.3 (where 4.5 would be
133 the estimate for an individual with mild disease breathing ambient air) to 1.6 with the patients
134 with critical disease having an estimate of 0.8 (median in severe group 3.8).

135

136 ***Ex vivo* assessment of memory T cell responses specific to SARS-CoV-2**

137 PBMCs were tested for responses to a panel of 423 overlapping peptides spanning the
138 SARS-CoV-2 proteome except ORF1, using *ex vivo* IFN- γ ELISpot assays. All overlapping
139 peptides were placed into two 2-dimensional peptide matrices: a total of 61 peptide pools
140 were tested, with 29 peptides in the first-dimension pools, as described in Supplementary
141 Table 1. The majority of the participants exhibited SARS-CoV-2 memory T cell responses to
142 at least one of the peptides. The overall distribution, magnitude and breadth of the IFN- γ
143 responses against all SARS-CoV-2 virus peptides are shown in Fig. 1. There was no
144 correlation between the T cell responses and the time that had elapsed from symptom
145 development (Supplementary Fig. 2). No *ex vivo* IFN γ -producing SARS-CoV-2-specific T
146 cell responses were observed in healthy volunteers, who were all sampled before any
147 chance of exposure, but in those with appropriate HLA types, T cell responses were
148 observed to influenza virus, EBV, CMV (FEC) using pools of known T cell epitopes as well
149 as PHA as positive controls (Supplementary Fig. 3). The breadth and magnitude of the T
150 cell responses varied considerably between individuals. T cell responses were detected
151 against epitopes distributed across a wide variety of virus proteins. Significantly higher
152 magnitude ($p=0.002$) and broader ($p=0.002$) overall T cell responses were observed in

153 severe cases in comparison with mild cases, in particular for responses to spike
154 (magnitude/breadth, $p=0.021/0.016$), membrane (magnitude/breadth, $p<0.001/p=0.033$),
155 ORF3 (magnitude/breadth, $p<0.001/0.001$) and ORF8 (magnitude/breadth, $p=0.011/0.014$)
156 proteins (Fig. 2).

157

158 **Correlation with spike specific antibody responses**

159 The relationship between spike-specific, and overall T cell responses in association with
160 spike-specific, receptor binding domain (RBD) and NP-specific antibody endpoint titres
161 (EPTs) was assessed (Fig. 3). There were significant correlations between (a) spike-specific
162 antibody titers and both overall T cell responses ($p<0.001/R=0.52$) and spike-specific T cell
163 responses ($p=0.001/R=0.51$); (b) RBD-specific antibody titers and both overall T cell
164 responses ($p<0.001/R=0.52$) and spike-specific T cell responses ($p<0.001/R=0.52$); and (c)
165 NP-specific antibody titers and both overall T cell responses ($p=0.002/R=0.47$) and spike-
166 specific T cell responses ($p=0.007/R=0.41$). However, there was no significant association
167 between NP-specific antibody titers and NP-specific T cell responses ($p=0.067/R=0.29$);
168 (Fig. 3a-c; and Supplementary Fig. 4). Moreover, significantly higher level of spike, RBD and
169 NP EPTs were observed in severe cases in comparison with mild cases (Fig. 3d). It was
170 noted that some individuals had low RBD-specific antibodies (Fig. 3b), yet had detectable
171 spike-specific antibodies (Fig. 3a), suggesting that antibodies were able to target non-RBD
172 regions of spike – these are under further investigation.

173

174 **Distribution of SARS-CoV-2-specific CD4⁺ and CD8⁺ memory T cell responses**

175 Having identified overall T cell responses to SARS-CoV-2 peptides, the responses detected
176 against positive peptide pools were characterized by flow cytometry for peptide recognition
177 by CD4⁺ or CD8⁺ T cell subsets and for intracellular production of IFN- γ , TNF- α and IL-2
178 after stimulation (Fig. 4a-b and Supplementary Fig. 5). A greater proportion of the T cell
179 responses to **spike** ($p=0.0268$) and M/NP ($p=0.02$) were contributed to by CD8⁺ T cells in

180 those with mild disease compared to those with severe disease (Fig. 4c, supplementary Fig.
181 6a)

182

183 **Evaluation of the polyfunctionality of T cells responding to SARS-CoV-2 peptides**

184 Multi-cytokine analysis revealed patterns of IFN γ , TNF α and IL-2 production by CD4 $^+$ and
185 CD8 $^+$ T cells in both mild and severe cases (Fig. 5a), For 22 individuals tested, both CD4 $^+$
186 and CD8 $^+$ antigen-specific-T cells produced least one of these three cytokines and others in
187 combination. CD8 $^+$ but not CD4 $^+$ T cells targeting different virus proteins showed different
188 cytokine profiles, with the M/NP-specific CD8 $^+$ T cells showing wider functionality than T cells
189 targeting spike protein ($p=0.0231$, Fig. 5b and supplementary Fig. 6b). Furthermore, there
190 were a greater proportion of multifunctional M/NP-specific CD8 $^+$ T cells compared to spike-
191 specific T cells in those that had mild disease ($p=0.0037$), but not in those that had severe
192 disease ($p=0.3823$). In contrast to observations seen in influenza virus infection¹⁹, we did
193 not observe significant differences in the cytotoxic potential (as indicated by expression of
194 the degranulation marker CD107a) in patients with mild and severe disease (Fig. 5c); and
195 we observed very few CD107a $^+$ CD4 $^+$ T cells overall, suggesting cytotoxic CD4 $^+$ T cells
196 might not be a major contributor to virus clearance.

197

198 **Identification of SARS-CoV-2 specific T cell peptides containing epitopes**

199 IFN γ ELISpot assays were performed with candidate peptides identified from the 2-
200 dimensional matrix analysis in 34 subjects. A total of 41 peptides containing SARS-CoV-2 T
201 cell epitope regions were recognized by COVID-19 convalescent subjects, 18 from spike, 10
202 from NP, 6 from membrane and 7 from ORF proteins. Strikingly, 6 dominant 18mer peptides
203 were recognised by 6 or more of 34 subjects tested (Table 1). NP-16 was recognised by
204 12/34 (35%) subjects tested and contained at least two epitopes which recognised by either
205 CD4 $^+$ T cells or CD8 $^+$ T cells.

206

207 M-24 was recognised by 16/34 subjects (47%) tested and contained one or more CD4⁺ T
208 cell epitopes. Peptide M-20 was recognised by 11/34 subjects tested (32%) and contained
209 one or more CD4⁺ T cell epitopes. 3 dominant spike peptides were also identified, with S-34
210 recognised by 10/34 subjects (29%) containing both CD4⁺ and CD8⁺ T cell epitopes, and a
211 further two spike peptides S-151 and S-174 were recognised by 8/34 and 6/34 subjects (24%
212 and 18%), both containing CD4⁺ T cell epitopes.

213

214 Those dominant responses were further confirmed by *ex-vivo* assays and by using cultured
215 short-term T cell lines. Supplementary Fig. 7 illustrates examples of FACS plots from
216 intracellular cytokine staining (ICS) when short-term T cell lines were stimulated with single
217 peptides containing epitopes. CD4⁺ T cells elicited strong responses against dominant spike
218 peptides and M peptides, whereas cells targeting two NP dominant peptides were CD8⁺ T
219 cells. The optimal epitopes within the long peptides recognized by dominant CD8⁺ T cells
220 and their HLA restriction, matched to the donor's HLA type, were predicted using the IEDB
221 analysis resource (<http://tools.iedb.org/mhci>). The best predicted epitope sequences are
222 shown in supplementary Table 2.

223

224 A set of previously defined SARS epitopes²⁰ with identical sequences to SARS-CoV-2 were
225 also tested by ELISpot assay (Supplementary table 3), Most of those peptides did not elicit
226 any positive responses in 42 COVID-19 recovered subjects, apart from two NP epitope
227 peptides (N-E-3 MEVTPSGTWL and N-E-11 LLNKHIDAYKTFPPTEPK) and one spike
228 epitope peptide (S-E-19 QLIRAAEIRASANLAATK) . N-E-11, which is identical to peptide
229 NP-51, shares the sequence with two other known HLA-A*0201 restricted SARS epitopes
230 (N-E-1 ILLNKHID and N-E-5 ILLNKHIDA). Interestingly, one of the responders to this
231 peptide did not carry the HLA-A*0201 allele (Table 1), indicating this peptide may contain a
232 different SARS-CoV-2 epitope presented by a different HLA molecule. Whereas these NP
233 epitopes are targeted by CD8⁺ T cells, we also detected a CD4⁺ T cell response targeting

234 SARS spike epitope S-E-19 which spans between the overlapping peptides of S-203 and S-
235 204. This peptide is known to be presented by HLA-DRB1*0401 in SARS infection.

236

237 The optimal peptide sequences and their HLA restrictions were confirmed by generating
238 short term T cell lines and clones, which were tested in ELIspot assays by co-culturing with
239 peptide loaded HLA matched and unmatched immortalized B lymphoblastoid cell lines
240 (BCLs) as previously described²¹. In total 6 CD8+ T cell epitopes restricted by HLA-A*0101,
241 A*0301, A*1101, B*0702, B*4001 and B*2705 were confirmed (Fig. 6a). HLA-peptide
242 pentamers were synthesized comprising 5 peptides bound to the appropriate HLA class I
243 molecules. T cell staining was verified by flowcytometry (Fig. 6b) and their phenotypes were
244 determined (Fig. 7). A pentameric HLA-A*0201 with the spike epitope reported
245 by Shomuradova *et al*²², was synthesised. Only one out of six HLA-A*0201-positive donors
246 showed detectable staining, but at a very low frequency. The majority of pentamer stained
247 SARS-Cov-2 specific CD8⁺ T cells exhibited central memory (20.7%±8.4%) or effector
248 memory phenotypes (50.3%±13.3%) (Fig. 7) and early (CD27+CD28+, 43.8%±20.9%) or
249 intermediate (CD27+CD28-, 49.3%±21.0%) differentiation phenotypes.

250

251 **Discussion**

252 This study demonstrates the presence of robust memory T cell responses specific for SARS-
253 CoV-2 in the blood of donors who have recovered from Covid-19. The broader and stronger
254 SARS-CoV-2 specific T cell responses in patients who had severe disease may be the result
255 of higher viral loads and may reflect a poorly functioning early T cell response that failed to
256 control the **virus, in addition to other factors such as direct virus-induced pathology**
257 **associated with larger viral inoculums or poorer innate immunity**. Alternatively, it is possible
258 that the T cell response was itself harmful and contributes to disease severity. Consistent
259 with recent reports from Grifoni *et al* and Sekine *et al*^{17,23}, a particularly high frequency of
260 spike protein-specific CD4⁺ T cell responses was observed in patients who had recovered
261 from COVID-19. This is very similar to influenza virus infection, where viral surface

262 hemagglutinin (HA) elicited mostly CD4⁺ T cell responses, whereas the majority of CD8⁺ T
263 cell responses were specific to viral internal proteins²⁴. Understanding the roles of different
264 subsets of T cells in protection or pathogenesis is a crucial question for COVID-19. The
265 timing and strength of the first T cell responses, could be critical in determining this balance
266 at an early stage of the infection.

267

268 Among the 41 peptides containing T cell epitopes that were identified in this study, six
269 immunodominant epitope groups (peptides) were frequently targeted by T cells in many
270 donors, including three in spike (29%, 24%, 18%), two in membrane protein (32%, 47%) and
271 one in nucleoprotein (35%). The immunodominant peptide regions identified here may
272 include multiple epitopes restricted by different HLAs (both class I and II, such as S-34 and
273 NP16) with immunodominance preferences imposed by the antigen processing pathways.
274 Whether or not these dominant responses play a role in immune protection merits further
275 investigation in larger prospective cohorts.

276

277 A higher proportion of CD8⁺ T cell responses was observed in mild disease, suggesting
278 the potential protective role of CD8⁺ T cell responses in mild disease or pathogenic role
279 of CD4⁺ T cell responses in severe disease which merits further investigation.

280

281 The majority of pentamer-binding CD8⁺ T cells were effector memory and central memory
282 with early and intermediate differentiation phenotypes, with functional potential on antigen
283 re-exposure. Because the number of donors studied was limited and they would likely show
284 diverse TCRs, peptide/MHC affinities and antigen sensitivities for the different epitopes, it
285 was not possible to make a detailed analysis comparing mild and severe cases. However,
286 the groundwork, including epitope identification, was laid for future studies that can address
287 this important issue.

288

289 Multiple strong dominant T cell responses were seen in study subjects, specific for the M
290 and NP proteins. Dominant epitope regions within NP (NP-16) were detected in 35% of
291 study subjects and M (M-20 and M24) were detected in 32% and 47%. In addition, a higher
292 proportion of multi-cytokine producing M/NP-specific compared to spike-specific CD8⁺ T
293 cells was observed in subjects who had recovered from mild disease. A similar trend was
294 also observed in severe cases, although was not significant possibly due to fewer cases.
295 These data strongly suggest NP and M have potential for inclusion within future vaccines so
296 as to stimulate strong effector T cell responses. Furthermore, T cells responding to these
297 antigens may be more cross-reactive¹⁸.

298

299 IFN- γ producing SARS-CoV-2 specific T cell responses were not observed in 16 healthy
300 unexposed volunteers differing from recently published reports by Grifoni *et al*¹⁷ and Braun
301 *et al*²⁵, both of which used peptide stimulated induction of activation markers (AIM) assays.
302 On the other hand, in a recent immunogenicity study of a recombinant adenovirus type-5
303 (Ad5) vectored COVID-19 vaccine human phase I trial in 108 volunteers without pre-
304 exposure to COVID-19), spike-specific T cell responses, measured IFN- γ ELISpot and
305 intracellular cytokine stimulation (ICS) assays, were not found before vaccination⁶. These
306 differences could result from differences in sensitivity of the detection methods, AIM versus
307 IFN- γ production assays. IFN- γ -ELISpot and ICS are well-established methods for
308 evaluating antigen specific T cells, used in different virus infections and vaccine studies, that
309 have direct functional relevance^{24, 26, 27, 28}. The AIM assay is more recently developed assay,
310 capable of detecting early responding T cells, that is independent of cytokine production.
311 Both methods are valid but differ in sensitivity and possible functional relevance. However, it
312 is also possible that different circulating coronaviruses have been previously present in the
313 different geographical populations studied, giving cross reactive responses in some regions
314 but not others, as suggested by Le Bert *et al*¹⁸. These T-cell cross reacting viruses could
315 include not only SARS-CoV-1 and human “common cold” coronaviruses, but also other

316 unknown coronaviruses of animal origin. It is also known that very sensitive assays can
317 detect not only pre-existing naïve antigen specific CD4⁺ T cells but also memory CD4⁺ T
318 cells. The latter are potentially primed by other microbes that cross react with viruses as
319 diverse as CMV, HIV-1 and Ebolavirus in most unexposed humans^{29, 30}. Therefore, similar
320 findings with SARS-CoV-2 peptides do not necessarily mean the T cells were primed by
321 previous infecting coronaviruses. Indeed, the implications of pre-existing cross-reactivity to
322 seasonal coronavirus and other viruses for COVID-19 immunity merits further detailed
323 investigation as nicely highlighted by *Sette A and Crotty S*³¹.

324

325 This study focuses on T cell responses in PBMC. There remains a lack of understanding of
326 memory T cells (T_{rm}) at the site of infection, which is likely providing the most potent
327 protection as observed in influenza virus infection³². It is possible that the hierarchy of
328 immunodominant circulating blood memory T cell pools may not exactly reflect that of T_{rm}
329 in the lung^{17, 33, 34}. Therefore, understanding the features of tissue resident memory T cells
330 and their association with disease severity will be critical and also merits further investigation.

331

332 Taken together, this study has demonstrated strong and broad SARS-CoV-2-specific CD4⁺
333 and CD8⁺ T cell responses in the majority of humans who had recovered from COVID-19.
334 The immunodominant epitope regions and peptides containing T cell epitopes identified in
335 this study will provide critical tools to study the contribution of SARS-CoV-19 specific T cells
336 in protection and immune pathology. Identification of non-spike dominant CD8⁺ T cell
337 epitopes, suggests the potential importance of including of non-spike protein such as NP, M
338 and ORFs into future vaccine designs.

339

340

341 **Materials and methods**

342

343 **Ethical Statement**

344 Patients were recruited from the John Radcliffe Hospital in Oxford, UK, between March and
345 May 2020 by identification of patients hospitalised during the SARS-COV-2 pandemic and
346 recruited into the Sepsis Immunomics and ISARIC Clinical Characterisation Protocols (IRAS
347 260007 and IRAS126600). Patients were sampled at least 28 days from the start of their
348 symptoms. Unexposed healthy adult donor samples were used from unrelated studies
349 undertaken between 2017-early 2019. Written informed consent was obtained from all
350 patients.

351

352 **Clinical definitions**

353 All patients were confirmed to have a test positive for SARS-CoV-2 using reverse
354 transcriptase polymerase chain reaction (RT-PCR) from an upper respiratory tract
355 (nose/throat) swab tested in accredited laboratories. The degree of severity was identified as
356 mild, severe or critical infection according to recommendations from the World Health
357 Organisation. Patients were classified as 'mild' if they did not require oxygen (that is, their
358 oxygen saturations were greater than 93% on ambient air) or if their symptoms were
359 managed at home. A large proportion of our mild cases were admitted to hospital for public
360 health reasons during the early phase of the pandemic even though they had no medical
361 reason to be admitted to hospital. Severe infection was defined as COVID-19 confirmed
362 patients with one of the following conditions: respiratory distress with RR>30/min; blood
363 oxygen saturation<93%; arterial oxygen partial pressure (PaO₂) / fraction of inspired O₂
364 (FiO₂) <300mmHg; and critical infection was defined as respiratory
365 failure requiring mechanical ventilation or shock; or other organ failures requiring admission
366 to ICU. Since the Severe classification could potentially include individuals spanning a wide
367 spectrum of disease severity ranging from patients receiving oxygen through a nasal
368 cannula through to non-invasive ventilation we also calculated the SaO₂/FiO₂ ratio at the

369 height of patient illness as a quantitative marker of lung damage. This was calculated by
370 dividing the oxygen saturation (as determined using a bedside pulse oximeter) by the
371 fraction of inspired oxygen (21% for ambient air, 24% for nasal cannulae, 28% for simple
372 face masks and 28, 35, 40 or 60% for Venturi face masks or precise measurements for non-
373 invasive or invasive ventilation settings). Patients not requiring oxygen with oxygen
374 saturations (if measured) greater than 93% on ambient air, or managed at home were
375 classified as mild disease. Viral swab Ct values were not available for all patients. In addition,
376 we have standardised all of our analyses to the days since symptom onset.

377

378 **Synthetic peptides**

379 A total of 423 15- to 18-mer peptides overlapping by 10 amino acid residues and spanning
380 the full proteome of the SARS-CoV-2 except ORF-1 (Supplementary Table 1) were designed
381 using software PeptGen (<http://www.hiv.lanl.gov/content/sequence/PEPTGEN/peptgen.html>)
382 and synthesized (purity >75%; Proimmune).

383 27 previously defined SARS epitopes²⁰ were also synthesised (Supplementary Table
384 2). Pools of Cytomegalovirus (CMV), Epstein-Barr virus (EBV) and influenza virus specific
385 epitope peptides and The human immunodeficiency viruses (HIV) gag were also used as
386 positive and negative controls.

387

388 **2-dimensional peptide matrix system**

389 The overlapping peptides spanning the SARS-CoV-2 were assigned into a 2-dimensional
390 matrix system in which each peptide was represented in 2 different peptide pools. Each
391 peptide pool contains no more than 16 individual peptides. The first dimension of the peptide
392 matrix system was designed so that peptides from different source proteins were separated
393 into different pools. (Supplemental Table 1).

394

395 ***Ex vivo* ELISpot assay**

396 IFN- γ ELISpot assays were performed using either freshly isolated or cryopreserved PBMCs
397 as described previously. No significant difference was observed between responses
398 generated by fresh or cryopreserved PBMCs as described previously^{24, 35}.

399

400 Overlapping peptides were pooled and then added to 200,000 PBMCs per test at the final
401 concentration of 2 μ g/mL for 16–18 h, the positive responses were confirmed by repeat
402 ELISPOT assays. To quantify antigen-specific responses, mean spots of the control wells
403 were subtracted from the positive wells, and the results expressed as spot forming units
404 (SFU)/10⁶ PBMCs. Responses were considered positive if results were at least three times
405 the mean of the negative control wells and >25SFU/10⁶PBMCs. If negative control wells
406 had >30SFU/10⁶ PBMCs or positive control wells (PHA stimulation) were negative, the
407 results were excluded from further analysis.

408

409 **Determination of plasma binding to trimeric spike, RBD and NP by ELISA**

410 MAXISORP immunoplates (442404; NUNC) were coated with 0.125 μ g of StrepMAB-Classic
411 (2-1507-001;iba) , blocked with 2% skimmed milk in PBS for one hour and then incubated
412 with 50 μ L of 5 μ g/mL soluble trimeric Spike 2 μ g/mL or 2% skim milk in PBS. After one hour,
413 50 μ L of serial two-fold dilutions of plasma, from 1:50 to 1:51200 in PBS containing 2%
414 skimmed milk were added followed by ALP-conjugated anti-human IgG (A9544; Sigma) at
415 1:10,000 dilution. The reaction was developed by the addition of PNPP substrate and
416 stopped with NaOH. The absorbance was measured at 405nm. Endpoint titers (EPTs) were
417 defined as reciprocal plasma dilutions that corresponded to two times the average OD
418 values obtained with mock. To determine EPTs to RBD and NP, immunoplates were coated
419 with 0.125 μ g of Tetra-His antibody (34670; QIAGEN) followed by 2 μ g/mL and 5 μ g/mL of
420 soluble RBD and NP, respectively.

421

422 **Intracellular cytokine staining (ICS)**

423 Intracellular cytokine staining was performed as described previously^{36,37}. Briefly, overnight
424 rested PBMCs were stimulated with pooled or individual peptides at a final concentration of
425 10µg/mL for 1 h in the presence of 2µg/mL monoclonal antibodies CD28 and CD49d, and
426 then for an additional 5h with GolgiPlug, GolgiStop and surface stained with PE-anti-CD107a.
427 Dead cells were labelled using LIVE/DEAD™ Fixable Aqua dye from Invitrogen; surface
428 markers including BUV395-anti-CD3, BUV737-anti-CD4, PerCP-Cy5.5-anti-CD8, BV510-
429 anti-CD14 (Biolegend), BV510-anti-CD16 (Biolegend) and BV510-anti-CD19 (Biolegend)
430 were stained. Cells were then washed, fixed with Cytotfix/Cytoperm™ and stained with PE-
431 Cy7-anti-IFN γ , APC-anti-TNF α (eBioscience), BV421-anti-IL-2 (Biolegend). Negative
432 controls without peptide-stimulation were run for each sample. All reagents were from BD
433 Bioscience unless otherwise stated. All samples were acquired on BD LSR Fortessa (BD
434 Biosciences) flow cytometer and analyzed using FlowJo™ v.10 software (FlowJo LLC). To
435 determine the frequency of different response patterns based on all possible combinations,
436 Boolean gates were created using IFN- γ , TNF- α and IL-2. Cytokine responses were
437 background subtracted individually prior to further analysis.

438

439 **Pentamer phenotyping**

440 Cryopreserved PBMCs were thawed as described above. A total of 1×10^6 live PBMCs were
441 labeled with peptide-MHC class I Pentamer-PE (Proimmune, UK) and incubated for 15 min
442 at 37°C. Dead cells were first labelled with LIVE/DEAD™ Fixable Aqua dye (Invitrogen) and
443 then with surface markers CD3-BUV395, CD8-PerCP.Cy5.5, CD14-BV510 (Biolegend UK),
444 CD16-BV510 (Biolegend UK), CD19-BV510 (Biolegend UK), CD28-BV711, CD27-APC-
445 R700, CD45RA-APC-H7 and CCR7-PE-Dazzel 594 (Biolegend UK). All reagents were from
446 BD Bioscience unless otherwise stated. All samples were acquired on BD LSR Fortessa (BD
447 Biosciences) flow cytometer and analyzed using FlowJo™ v.10 software (FlowJo LLC).

448

449 **Generating short-term T cell lines**

450 Short-term SARS-CoV-2-specific T cell lines were established as previously described³⁵.
451 Briefly, 3×10^6 to 5×10^6 PBMCs were pulsed as a pellet for 1 h at 37°C with 10 µM of
452 peptides containing T cell epitope regions and cultured in R10 at 2×10^6 cells per well in a
453 24-well Costar plate. IL-2 was added to a final concentration of 100U/mL on day 3 and
454 cultured for further 10 -14 days.

455

456 **Statistical analysis**

457 Statistical analysis was performed with IBM SPSS Statistics 25 and Fig.s were made with
458 GraphPad Prism 8. Chi-square tests were used to compare ratio difference between two
459 groups. After testing for normality using Kolmogorov-Smirnov test, Independent-samples *t*
460 test or Mann-Whitney U test was employed to compare variables between two groups.
461 Correlations were performed via Spearman's rank correlation coefficient. Statistical
462 significance was set at * $P < 0.05$, ** $P < 0.01$, *** $P < 0.001$ and **** $P < 0.0001$. All the tests were
463 2-tailed.

464

465 **Data availability**

466 The data that support the findings of this study are available from the corresponding author
467 upon request.

468

469

470

471 **Acknowledgments**

472 We are grateful to all of the participants for donating their samples and data for these
473 analyses, and the research teams involved in the consenting, recruitment and sampling of
474 these participants. We acknowledge the support of ISARIC4C Investigators.

475

476 This work is supported by UK Medical Research Council; Chinese Academy of Medical
477 Sciences (CAMS) Innovation Fund for Medical Sciences (CIFMS), China (grant number:

478 2018-I2M-2-002); The National Institute for Health Research [award CO-CIN-01]; the
479 Medical Research Council [grant MC_PC_19059] ; the National Institute for Health
480 Research Health Protection Research Unit (NIHR HPRU) in Emerging and Zoonotic
481 Infections at University of Liverpool in partnership with Public Health England (PHE)[NIHR
482 award 200907]; Wellcome Trust and Department for International Development
483 [215091/Z/18/Z]; the Bill and Melinda Gates Foundation [OPP1209135]. The study is also
484 funded by the NIHR Oxford Biomedical Research Centre and Clinical Research Network;
485 and National Institutes of Health, National Key R&D Program of China(2020YFE0202400),
486 National Institute of Allergy and Infectious Disease (Consortium for HIV/AIDS Vaccine
487 Development UM1 AI 144371 (PB and AMcM) and R01 AI 118549 (PB).

488

489 The views expressed are those of the authors and not necessarily those of the Department
490 of Health and Social Care, DID, NIHR, MRC, Wellcome Trust or PHE.

491 **Author Contribution:** TD and GO conceptualized the project, TD, YP designed and
492 supervised T cell experiments, JM and GS designed antibody experiments; YP, GL, XY,
493 ZY,DD performed all T cell experiments; WD, JM, PS, CL, CLC, JSC, YZ, DS, GP, JG,
494 FA,OB,DH, BW and DSK performed Spike, RBD and NP EPTs experiments; TR performed
495 HLA typing; JK, AM, TL, RL, PK, LT, TDS, MGS, CC, SM, KB, PO established clinical
496 cohorts and collected clinical sample and data; KS, PT, PZ, CD, JR, PS, PS, DW, UR, YLC,
497 WP, PB, BK, JF, AA, SD, MS, EB, GK, PG, YZ, RJ, LPH provided critical reagents and
498 technical assistance; YP, GL, XY, ZY,DD, WD, PZ, JM and analysed data, TD wrote the
499 original draft. GO, JK, AM, PK, PO, GS, RC, PS, CC reviewed and edited the manuscript
500 and Figures.

501 All authors declare no competing interest

502

503

505 **References**

506

- 507 1. Fehr A.R., P.S. Coronaviruses: An Overview of Their Replication and Pathogenesis. *In:*
508 *Maier H., Bickerton E., Britton P. (eds) Coronaviruses. Methods in Molecular Biology*
509 **vol 1282.**
510
- 511 2. Perlman, S. & Netland, J. Coronaviruses post-SARS: update on replication and
512 pathogenesis. *Nat Rev Microbiol* **7**, 439-450 (2009).
513
- 514 3. Xu, Z. *et al.* Pathological findings of COVID-19 associated with acute respiratory
515 distress syndrome. *Lancet Respir Med* **8**, 420-422 (2020).
516
- 517 4. Guan, W.J. *et al.* Clinical Characteristics of Coronavirus Disease 2019 in China. *N Engl*
518 *J Med* (2020).
519
- 520 5. Yu, J. *et al.* DNA vaccine protection against SARS-CoV-2 in rhesus macaques. *Science*
521 (2020).
522
- 523 6. Zhu, F.C. *et al.* Safety, tolerability, and immunogenicity of a recombinant adenovirus
524 type-5 vectored COVID-19 vaccine: a dose-escalation, open-label, non-randomised,
525 first-in-human trial. *Lancet* **395**, 1845-1854 (2020).
526
- 527 7. van Doremalen, N. *et al.* ChAdOx1 nCoV-19 vaccination prevents SARS-CoV-2
528 pneumonia in rhesus macaques. *bioRxiv*, 2020.2005.2013.093195 (2020).
529
- 530 8. Folegatti, P.M. *et al.* Safety and immunogenicity of the ChAdOx1 nCoV-19 vaccine
531 against SARS-CoV-2: a preliminary report of a phase 1/2, single-blind, randomised
532 controlled trial. *Lancet* (2020).
533
- 534 9. St John, A.L. & Rathore, A.P.S. Adaptive immune responses to primary and secondary
535 dengue virus infections. *Nat Rev Immunol* **19**, 218-230 (2019).
536
- 537 10. Huang, C. *et al.* Clinical features of patients infected with 2019 novel coronavirus in
538 Wuhan, China. *Lancet* **395**, 497-506 (2020).
539
- 540 11. Liao, M. *et al.* Single-cell landscape of bronchoalveolar immune cells in patients with
541 COVID-19. *Nat Med* (2020).
542
- 543 12. chen, y. *et al.* The Novel Severe Acute Respiratory Syndrome Coronavirus 2 (SARS-
544 CoV-2) Directly Decimates Human Spleens and Lymph Nodes. *medRxiv*,
545 2020.2003.2027.20045427 (2020).
546
- 547 13. Diao, B. *et al.* Reduction and Functional Exhaustion of T Cells in Patients With
548 Coronavirus Disease 2019 (COVID-19). *Front Immunol* **11**, 827 (2020).
549

- 550 14. Pereira, B.I. *et al.* Sestrins induce natural killer function in senescent-like CD8(+) T
551 cells. *Nat Immunol* **21**, 684-694 (2020).
552
- 553 15. Ni, L. *et al.* Detection of SARS-CoV-2-Specific Humoral and Cellular Immunity in
554 COVID-19 Convalescent Individuals. *Immunity* (2020).
555
- 556 16. Hayward, A.C. *et al.* Natural T Cell-mediated Protection against Seasonal and
557 Pandemic Influenza. Results of the Flu Watch Cohort Study. *Am J Respir Crit Care*
558 *Med* **191**, 1422-1431 (2015).
559
- 560 17. Grifoni, A. *et al.* Targets of T Cell Responses to SARS-CoV-2 Coronavirus in Humans
561 with COVID-19 Disease and Unexposed Individuals. *Cell* **181**, 1489-1501 e1415 (2020).
562
- 563 18. Le Bert, N. *et al.* SARS-CoV-2-specific T cell immunity in cases of COVID-19 and SARS,
564 and uninfected controls. *Nature* (2020).
565
- 566 19. Wilkinson, T.M. *et al.* Preexisting influenza-specific CD4+ T cells correlate with
567 disease protection against influenza challenge in humans. *Nat Med* **18**, 274-280
568 (2012).
569
- 570 20. Ahmed, S.F., Quadeer, A.A. & McKay, M.R. Preliminary Identification of Potential
571 Vaccine Targets for the COVID-19 Coronavirus (SARS-CoV-2) Based on SARS-CoV
572 Immunological Studies. *Viruses* **12** (2020).
573
- 574 21. Ogg, G.S. *et al.* Four novel cytotoxic T-lymphocyte epitopes in the highly conserved
575 major homology region of HIV-1 Gag, restricted through B*4402, B*1801, A*2601,
576 B*70 (B*1509). *AIDS* **12**, 1561-1563 (1998).
577
- 578 22. Shomuradova, A.S. *et al.* SARS-CoV-2 epitopes are recognized by a public and diverse
579 repertoire of human T-cell receptors. *medRxiv*, 2020.2005.2020.20107813 (2020).
580
- 581 23. Sekine, T. *et al.* Robust T cell immunity in convalescent individuals with
582 asymptomatic or mild COVID-19. *bioRxiv*, 2020.2006.2029.174888 (2020).
583
- 584 24. Lee, L.Y. *et al.* Memory T cells established by seasonal human influenza A infection
585 cross-react with avian influenza A (H5N1) in healthy individuals. *J Clin Invest* **118**,
586 3478-3490 (2008).
587
- 588 25. Braun, J. *et al.* Presence of SARS-CoV-2 reactive T cells in COVID-19 patients and
589 healthy donors. *medRxiv*, 2020.2004.2017.20061440 (2020).
590
- 591 26. Li, C.K. *et al.* T cell responses to whole SARS coronavirus in humans. *J Immunol* **181**,
592 5490-5500 (2008).
593
- 594 27. Powell, T.J. *et al.* Identification of H5N1-specific T-cell responses in a high-risk cohort
595 in vietnam indicates the existence of potential asymptomatic infections. *J Infect Dis*
596 **205**, 20-27 (2012).

597
598 28. Dong, T. *et al.* Extensive HLA-driven viral diversity following a narrow-source HIV-1
599 outbreak in rural China. *Blood* **118**, 98-106 (2011).
600
601 29. Su, L.F. & Davis, M.M. Antiviral memory phenotype T cells in unexposed adults.
602 *Immunol Rev* **255**, 95-109 (2013).
603
604 30. Champion, S.L. *et al.* Proteome-wide analysis of HIV-specific naive and memory CD4(+)
605 T cells in unexposed blood donors. *J Exp Med* **211**, 1273-1280 (2014).
606
607 31. Sette, A. & Crotty, S. Pre-existing immunity to SARS-CoV-2: the knowns and
608 unknowns. *Nat Rev Immunol* (2020).
609
610 32. Pizzolla, A. *et al.* Resident memory CD8(+) T cells in the upper respiratory tract
611 prevent pulmonary influenza virus infection. *Sci Immunol* **2** (2017).
612
613 33. Turner, D.L. *et al.* Lung niches for the generation and maintenance of tissue-resident
614 memory T cells. *Mucosal Immunol* **7**, 501-510 (2014).
615
616 34. Yoshizawa, A. *et al.* TCR-pMHC encounter differentially regulates transcriptomes of
617 tissue-resident CD8 T cells. *Eur J Immunol* **48**, 128-150 (2018).
618
619 35. Peng, Y. *et al.* Boosted Influenza-Specific T Cell Responses after H5N1 Pandemic Live
620 Attenuated Influenza Virus Vaccination. *Front Immunol* **6**, 287 (2015).
621
622 36. Lillie, P.J. *et al.* Preliminary assessment of the efficacy of a T-cell-based influenza
623 vaccine, MVA-NP+M1, in humans. *Clin Infect Dis* **55**, 19-25 (2012).
624
625 37. de Silva, T.I. *et al.* Correlates of T-cell-mediated viral control and phenotype of CD8(+)
626 T cells in HIV-2, a naturally contained human retroviral infection. *Blood* **121**, 4330-
627 4339 (2013).
628
629
630
631
632
633
634
635
636
637

639 **Table 1 Peptides containing T cell epitopes**

	Peptide	Position	Amino Acid Sequence	CD4/CD8 Response	No of subjects responded
Spike	S-34	166-180	CTFEYVSQPFLMDLE	4/8	<u>10</u>
(n=18)	S-39	191-205	EFVFNIDGYFKIYS	na	1
	S-42	206-230	KHTPINLVRDL PQGF	na	1
	S-43	211-225	NLVRDLPQGF SALEP	na	1
	S-71	351-365	YAWNKRISNCVADY	4	1
	S-77	381-395	GVSPTKLNDLCFTNV	4	1
	S-90	446-460	GGNYN YLRLFRKSN	na	1
	S-91	451-465	YLRLFRKSN LKPFE	na	1
	S-103	506-520	VVLSFELLHAPATVC	4	1
	S-106	526-540	GPKKSTNLVKNKCVN	8	1
	S-145	721-735	SVTTEILPVSMTKTS	na	1
	S-150	746-760	STECSN LLLQYGSFC	na	1
	S-151	751-765	NLLLQYGSFC TQLNR	<u>4</u>	<u>8</u>
	S-161	801-815	NFSQILPDPSPSKR	<u>4</u>	2
	S-174	866-880	TDEMQYTSALLAG	<u>4</u>	<u>6</u>
	S-235	1171-1185	GINASVWNIQKEIDR	na	1
	S-240	1196-1210	LIDLQELGKYEQYI	na	1
	S-242	1206-1220	YEQYIKWPWYIWLGF	na	1
	NP-1	1-17	MSDNGPQNQRNAPRITF	8	3
	NP-2	8-25	QRNAPRITF GGPSDSTG	8	3
NP	NP-12	82-95	DQIGYYRRATRRIR	na	1
(n=10)	NP-15	101-113	MKDLSRWYFYLL	na	1
	NP-16	104-121	LSPRWYFYLLGTGPEAGL	4/8	<u>12</u>
	NP-46	313-330	AFFGMSRIGMEVTPSGTW	na	1
	NP-47	321-338	GMEVTPSG TWLTYTGAIK	na	1
	NP-48	329-346	TWLTYTGAIK LDDKDPNF	4	2
	NP-50	344-361	PNFKDQVILLNKHIDAYK	4	1
	NP-51	352-369	LLNKHIDAYK TFPTEPK	8	3
	M19	133-150	LLESELVIGAVILRGHLR	na	3
M	M-20	141-158	GAVILRGHLRIAGHHLGR	4	<u>11</u>
(n=6)	M-21	149-166	LRIAGHHLGR CDIKDLPK	na	3
	M-23	165-181	PKEITVATSRTLSYYKL	na	3
	M-24	172-188	TSRTLSYYKL GASQRVA	4	<u>16</u>
	M-28	201-218	IGNYKLNTHSSSSDNIA	na	1
ORFs	ORF-3a-20	145-160	YFLCWHTNCYDYCIPY	na	1
(n=7)	ORF-3a-27	198-215	KDCVVLHSYFTSDYQLY	na	3
	ORF-3a-28	206-225	YFTSDYQLY STQLSTDTGV	8	4
	ORF-3a-30	224-243	GVEHVTFIYNKIVDEPEEH	na	1
	ORF-7a-2	9-25	LITLATCELYHYQECVR	na	3
	ORF-7a-7	46-63	FHPLADNKFALTCFSTQF	na	1
	ORF-7a-10	69-86	DGVKHVYQLRARSVSPKL	4	1

641 Red highlights the overlaps of two adjacent peptides recognised by same subjects; Bold
642 indicates multiple donor responders; Peptides with underline are the 6 immunodominant
643 peptides. na: not available

644 Figure Legends

645 **Fig. 1: Memory T cell responses specific to SARS-CoV-2 virus proteins in 42**
646 **convalescent SARS-CoV-2-infected patients.** 28 individuals had mild symptoms while 14
647 showed severe symptoms. PBMC were isolated and IFN γ production was detected by
648 ELISpot after incubation with SARS-CoV-2 peptides. a) Magnitude of IFN γ T cell responses
649 from each individual. Each bar shows the total T cell responses of each individual specific to
650 all the SARS-CoV-2 protein peptides tested. Each colored segment represents the source
651 protein corresponding to peptide pools eliciting IFN γ T cell responses. b) Breadth of T cell
652 responses from each individual. The breadth of T cell responses was calculated by the
653 number of peptide pools in the first-dimension (total 29) cells responded to SFU spot forming
654 units

655

656 **Fig. 2: Comparison of magnitude and breadth of T cell response specific to each viral**
657 **protein between convalescent patients with mild symptoms and severe symptoms.**

658 PBMCs were isolated and IFN γ production was detected by ELISpot after incubation with
659 SARS-CoV-2 peptides. a) and b) illustrate the magnitude and the breadth of T cell response
660 against each viral protein between the groups with mild symptoms (n=28) and with severe
661 symptoms (n=14), respectively. Data are presented as median with interquartile range.
662 Mann-Whitney test was used for the analysis and two-tailed p value was calculated. *P<0.05,
663 **P<0.01, ***P<0.001. SFU spot forming units;

664

665 **Fig. 3: Correlation of T cell responses against SARS-CoV-2 with Spike, RBD and NP-**
666 **specific antibody responses.** a) EPTs-spike b) EPTs-RBD and c) EPTs-NP in association

667 with overall T cell responses. Red dots represent the patients with severe symptoms
668 whereas the mild cases are shown as black dots. n=42. Spearman's rank correlation
669 coefficient was used for the correlation analysis. d) Comparison of EPT-spike (p<0.0001),
670 EPT-RBD (p<0.0001) and EPT-NP (p=0.0004) with mild symptoms (n=28) and severe

671 symptoms (n=14). Data are presented as median with interquartile range and Mann-Whitney
672 test was used for comparison. Two-tailed p value was calculated. *** P<0.001; **** P<0.0001

673 EPT: Endpoint titer

674

675 **Fig. 4: Distribution of SARS-CoV-2-specific CD4⁺ and CD8⁺ memory T cell responses**

676 Cytokine producing T cells were detected by ICS after incubation with SARS-CoV-2 peptides.

677 a) and b) FACS plots represent CD4⁺T cell and CD8⁺ T cells expressing IFN γ (x-axis), TNF α
678 (y-axis) and/or IL-2 (y-axis) upon stimulation with respective SARS-CoV-2 peptide pools in

679 examples of mild and severe cases. c) Comparison of relative proportion of SARS-CoV-2

680 peptide pool-reactive CD8⁺ T cells between mild and severe cases. The SARS-CoV-2

681 peptide pool-reactive CD4⁺ or CD8⁺ T cells were identified with at least one of the three

682 cytokines detected: IFN γ , TNF α and IL-2. The frequencies of SARS-CoV-2 peptide pool-

683 reactive CD4⁺ or CD8⁺ T cells were over 0.05% of CD4⁺ or CD8⁺ T cells, respectively.

684 Cytokine responses were background subtracted individually prior to further analysis. Data

685 shown are as median from 14 subjects with history of mild symptoms and 8 with severe

686 symptoms. Mann-Whitney test was used for the analysis. Two-tailed p value was calculated.

687 * P<0.05

688

689 **Fig. 5: Cytokine profile of SARS-Cov-2-specific T cells.** Cytokine production of SARS-

690 Cov-2-specific T cells was assessed by intracellular cytokine staining after incubation with

691 SARS-CoV-2 peptides. a) Pie charts represent the relative proportions of CD4⁺ or CD8⁺ T

692 cells producing, and the relative proportion of T cells producing one, two and three cytokines

693 IFN- γ , TNF α and IL-2. Different colored segments represented different pattern of cytokine

694 production. b) Comparison of the frequency of multifunctional CD8⁺ T cells targeting Spike

695 and M/NP. The open circles and squares represent T cell responses in mild cases and

696 severe cases, respectively. c) The relative frequencies of CD4⁺ and CD8⁺ T cells expressing

697 CD107a after antigen-stimulation. Data shown are from 14 subjects with mild symptoms and

698 8 with severe symptoms. Mann-Whitney test was used for the analysis. * P<0.05, **P<0.01

699

700 **Fig. 6: Defined SARS-CoV-2-specific CD8 epitopes.** a) List of identified optimal CD8
701 epitopes; b) Examples of peptide-MHC Class I pentamers staining ex-vivo with PBMCs
702 (HLA-B0702, B4001, A1101, A0101 and A0201) or with cultured cell lines (A0301).

703

704 **Fig. 7: Memory phenotype and differentiation status of SARS-CoV-2-specific CD8+ T**
705 **cells.** PBMC were isolated and stained with peptide-MHC class I Pentameric complexes and
706 markers of T cell memory and differentiation. a) Representative FACS plots of gating for
707 different cell subsets b) and c) Expression of memory markers (CCR7 and CD45RA) and
708 differentiation markers (CD27 and CD28) on CD8⁺ Pentamer+ T cells, respectively (N= 7
709 donors).

Figure 1

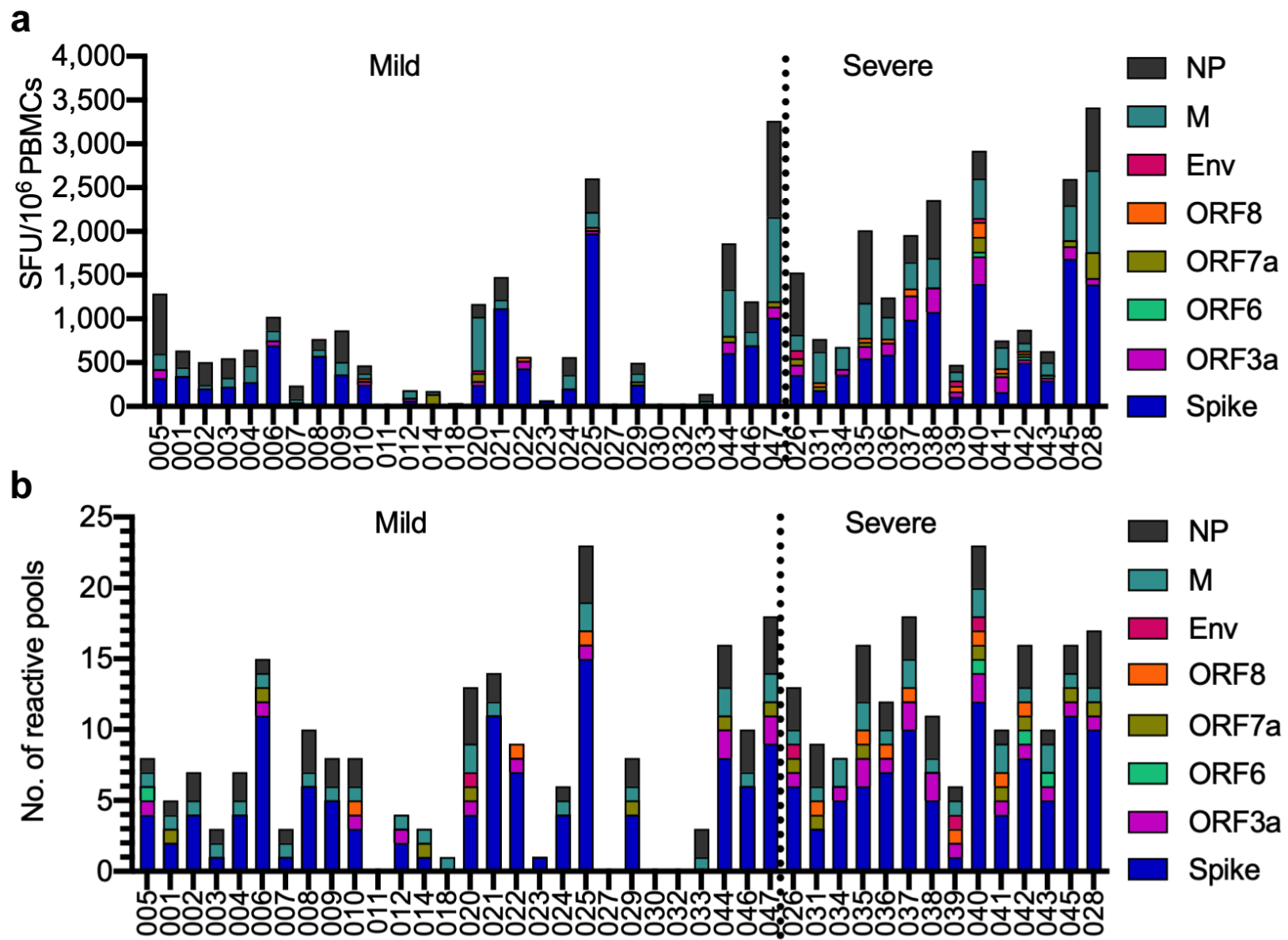


Figure 2

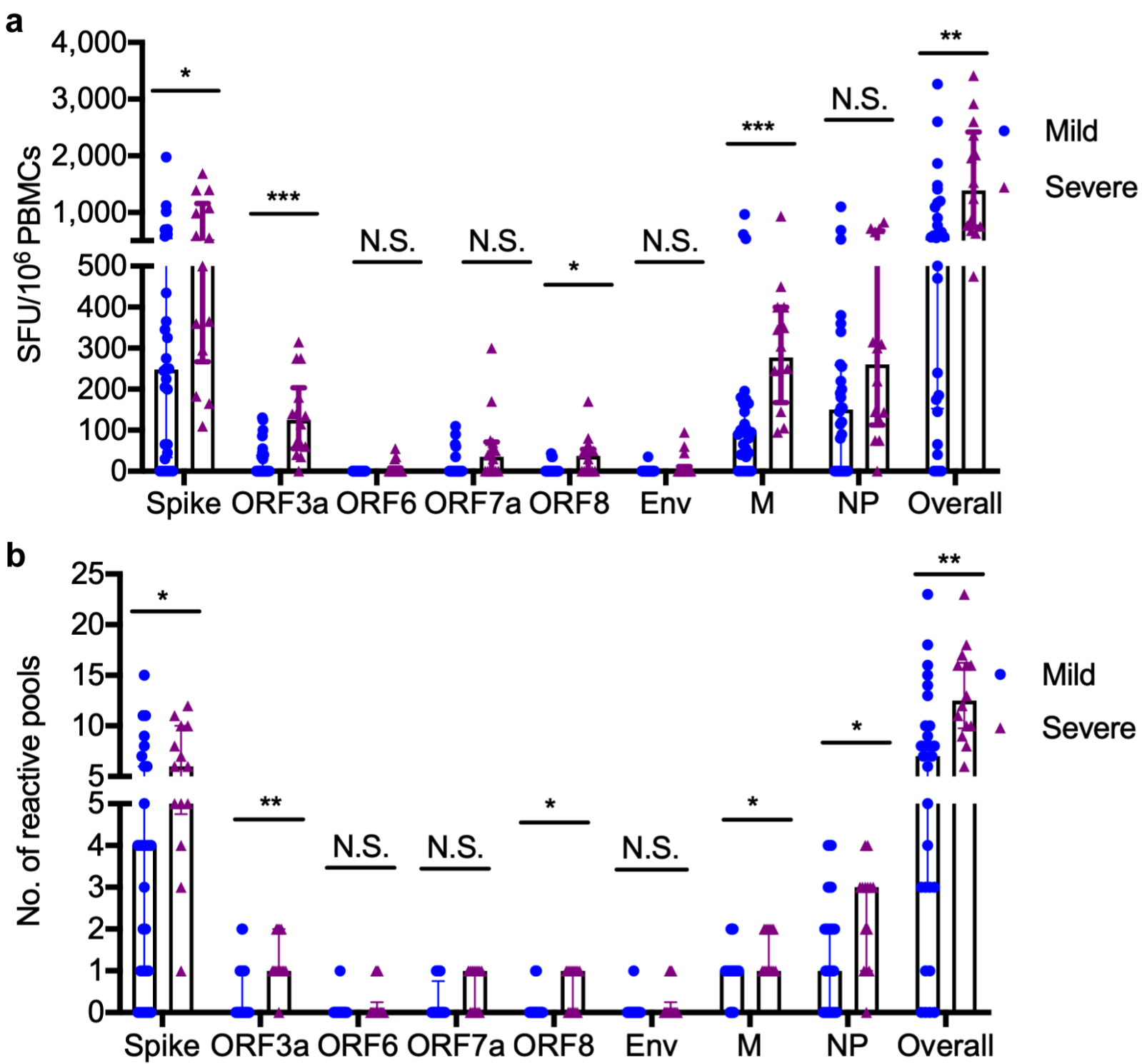


Figure 3

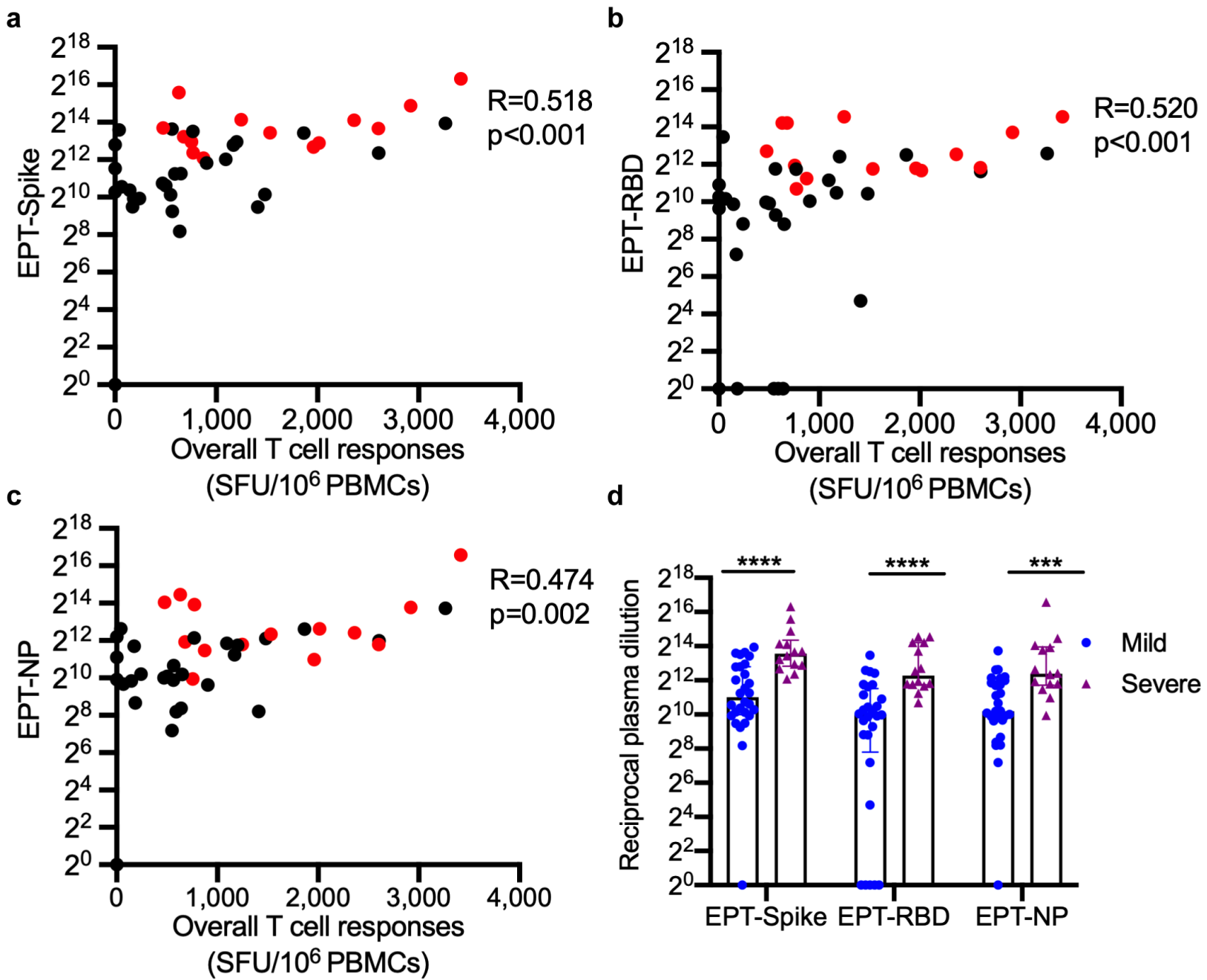


Figure 4

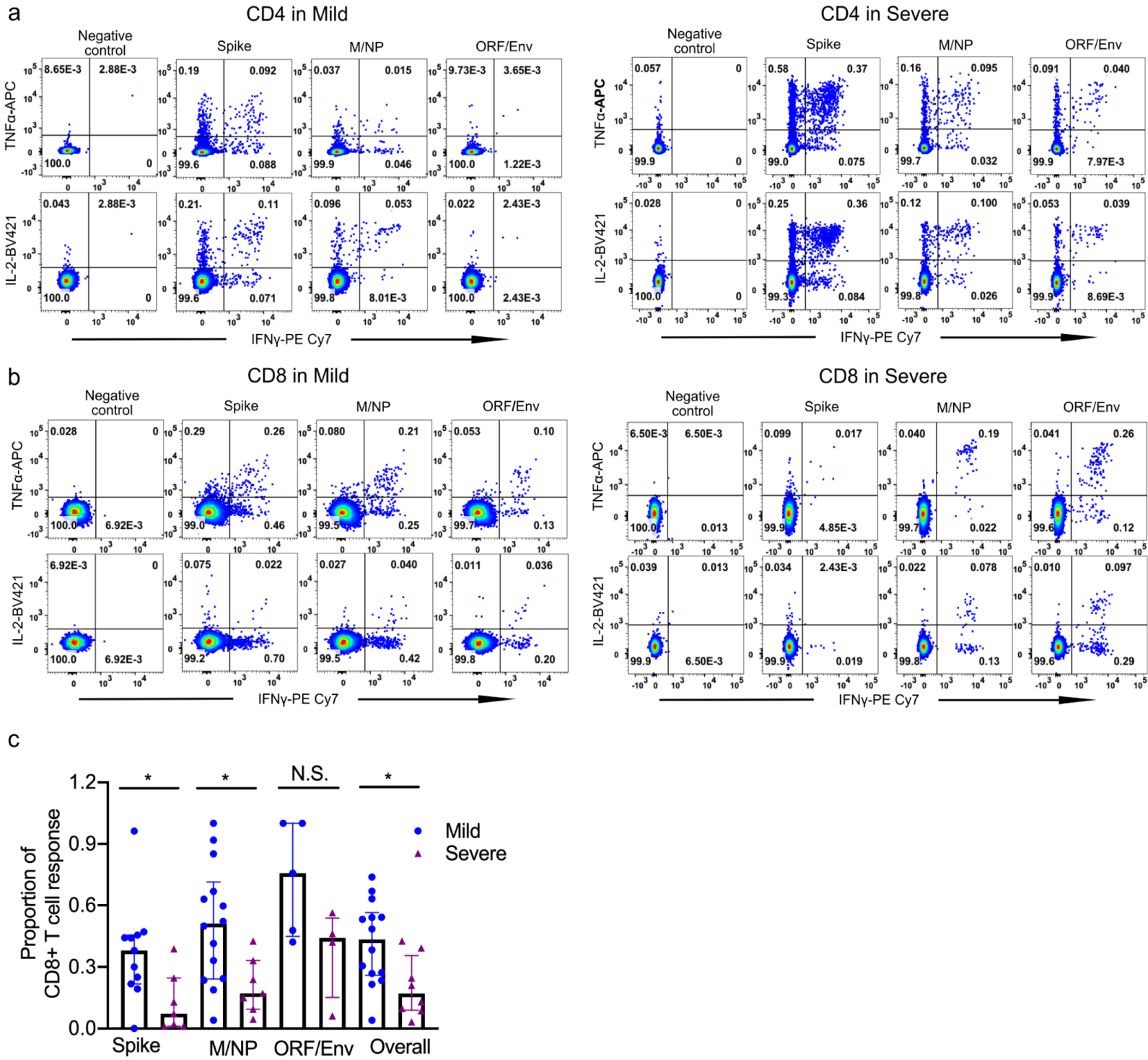


Figure 5

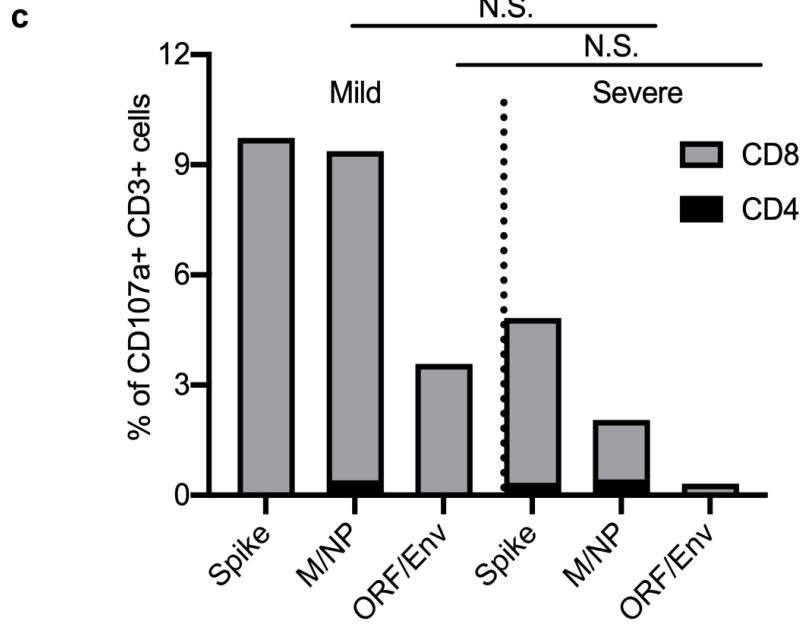
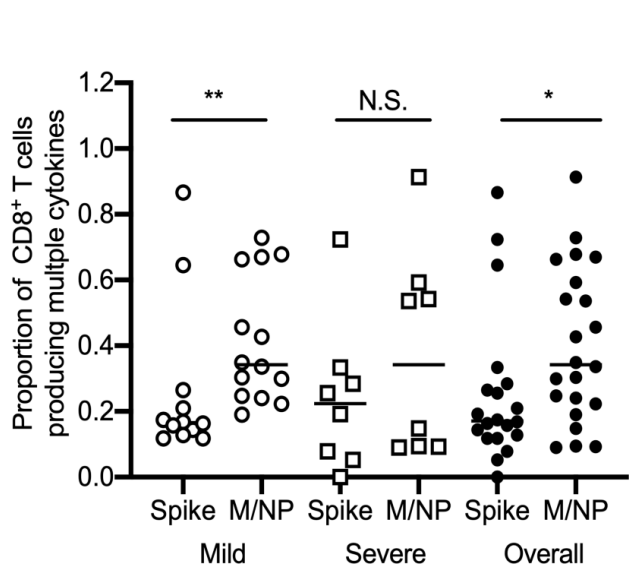
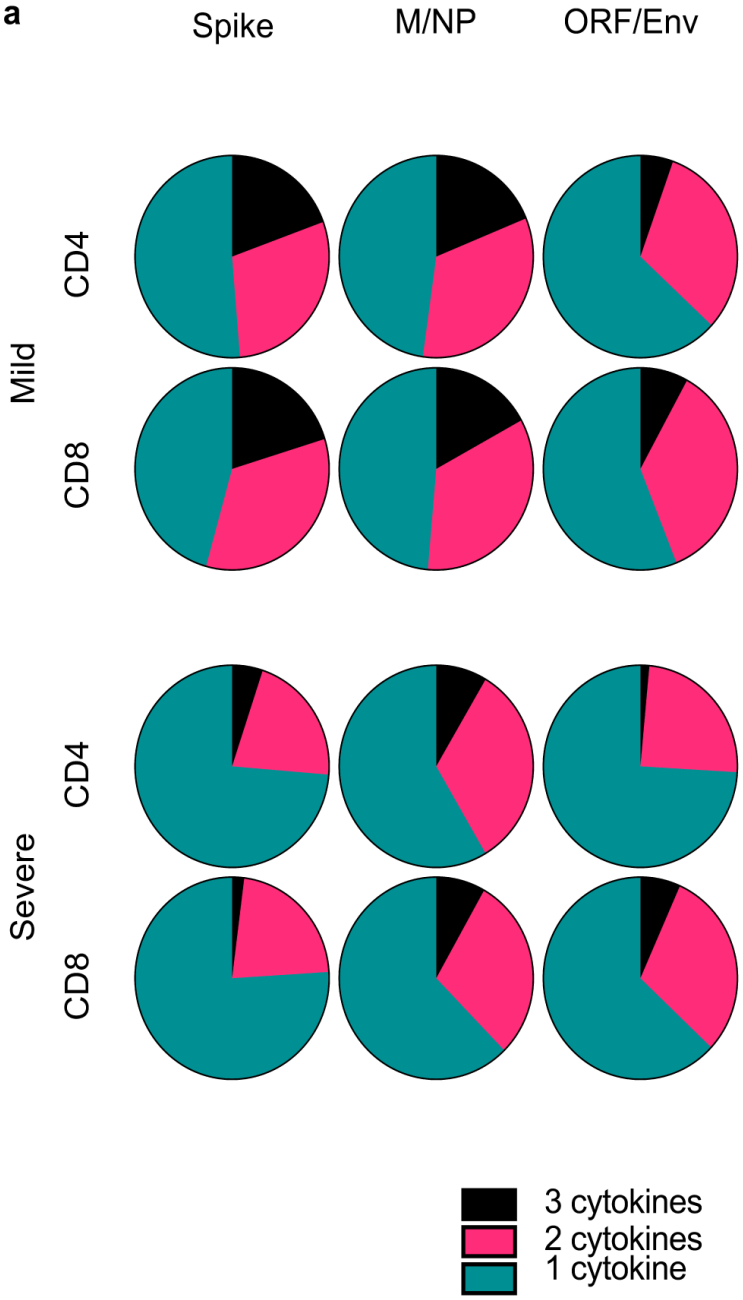


Figure 6

a

Protein	Position	Epitope sequence	HLA Restriction
NP	9-17	QRNAPRITF	B*2705
	105-113	SPRWYFYYL	B*0702
	322-331	MEVTPSGTWL	B*4001
	362-370	KTFPPTEPK	A*0301
	362-370	KTFPPTEPK	A*1101
ORF3a	207-215	FTSDYYQLY	A*0101
Spike	269-277	YLQPRTFLL	A*0201

b

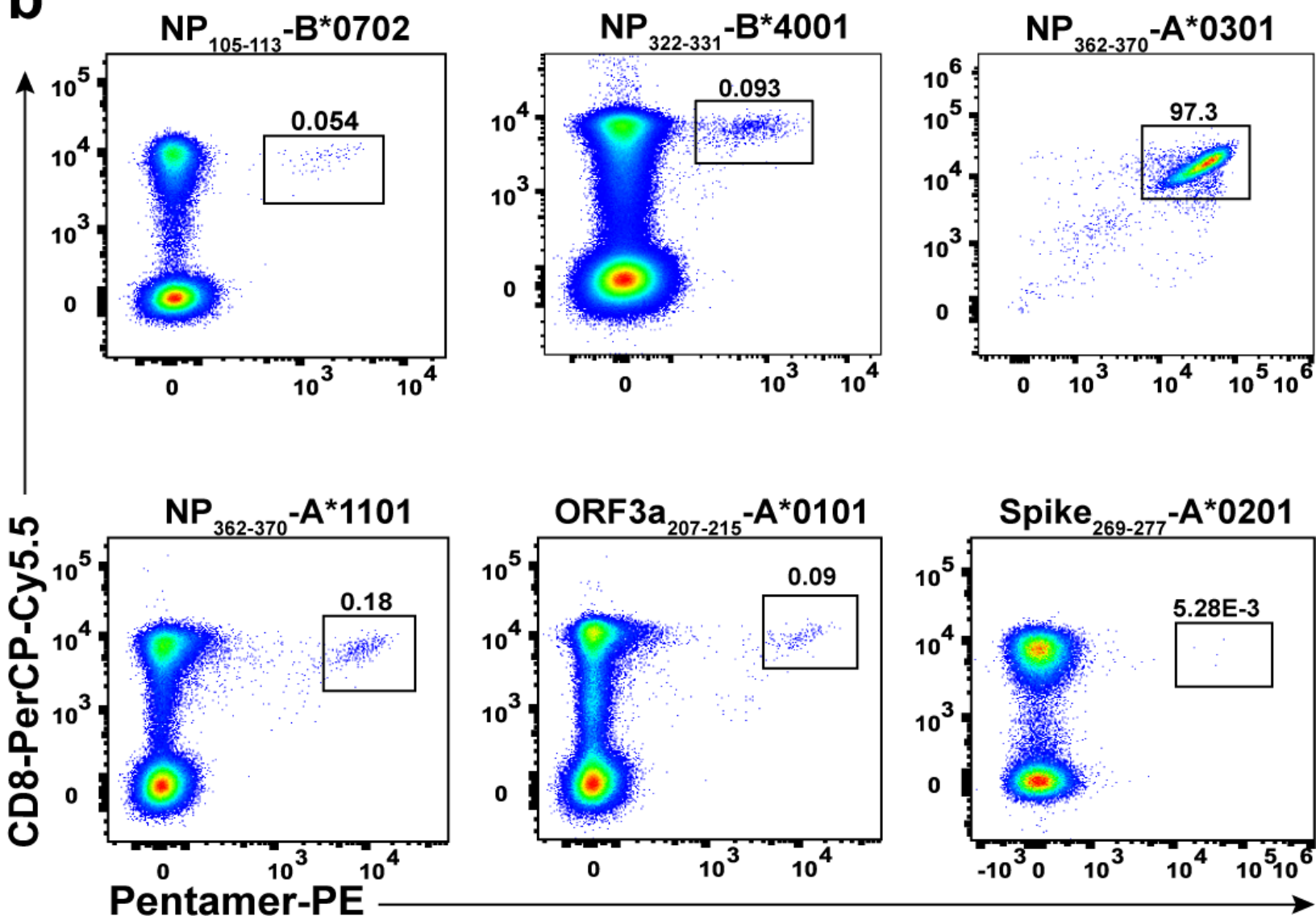
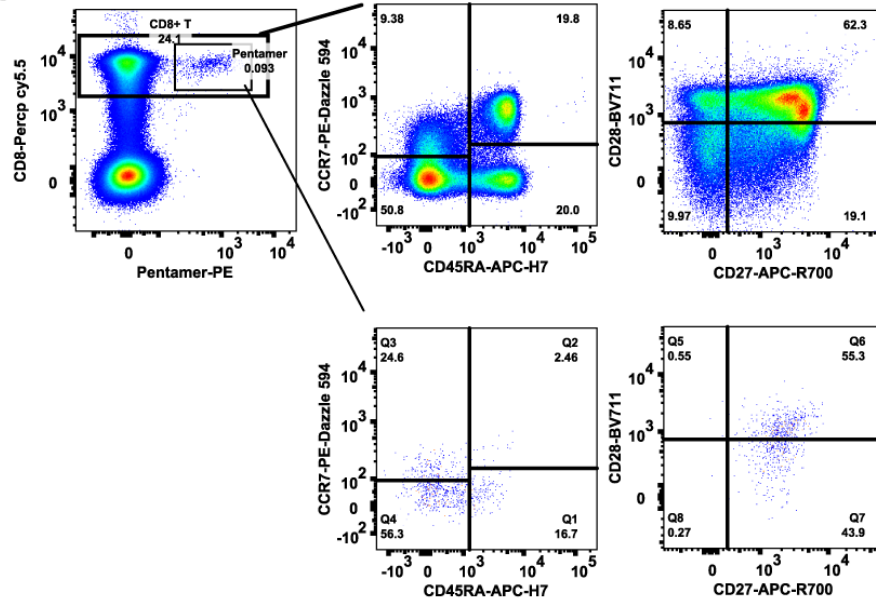
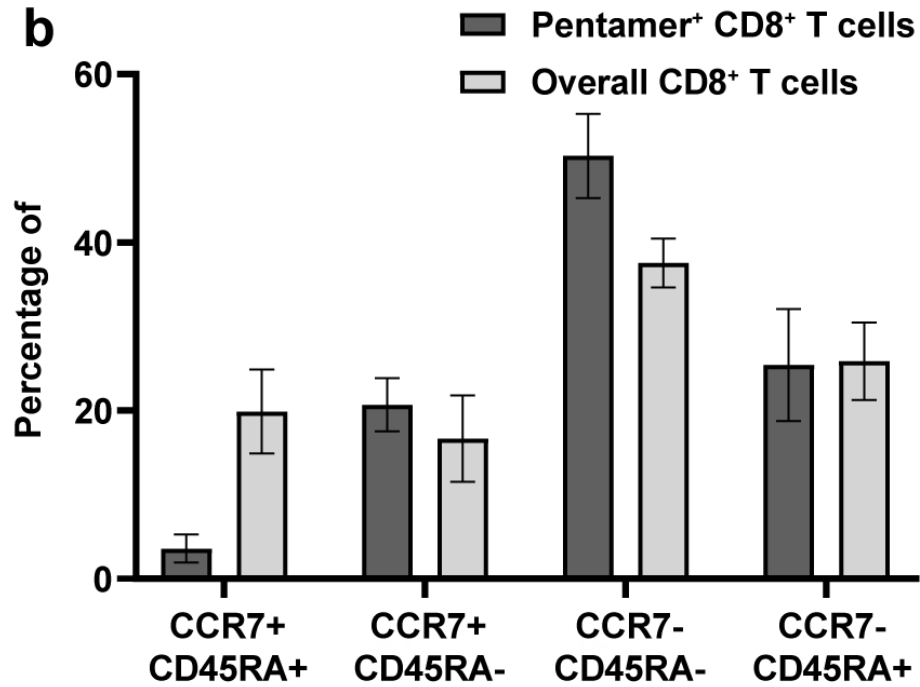


Figure 7

a



b



c

